Split and Merge of Left–Right Circular Polarized Light through Coupled Magnetic Resonators

Jijun Wang[a], Jing Cao[a], Min Zhu[a], Zhipan Zhu[a], and Yun-tuan Fang[b]

[a] Faculty of Science, Jiangsu University, Zhenjiang, 212013, P. R. China
[b] School of Computer Science and Telecommunication Engineering, Jiangsu University, Zhenjiang, 212013, P. R. China

Reprint requests to J. W.; E-mail: wjj4461@ujs.edu.cn

Z. Naturforsch. **67a,** 491 – 497 (2012) / DOI: 10.5560/ZNA.2012-0051
Received January 11, 2012 / revised May 7, 2012

In order to obtain the means to control light polarization, we designed a structure of coupled magnetic resonators and studied its transmission properties by the 4×4 transfer matrix method. The incidence of linearly polarized light results in two transmission resonant peaks of left-handed circular polarization at shorter wavelengths and two transmission resonant peaks of right-handed circular polarization at longer wavelengths, respectively. Through adjusting the magnetizations, the inner left-handed circular polarization and right-handed circular polarization can be merged into one linear polarization, while the two outside resonant peaks keep their circular polarization. The polarized direction of the output linearly polarized light can be controlled by the polarized direction of incidence light. The incidence light with one polarization can output light with three kinds of polarizations through the designed structure.

Key words: Light Polarizations; Coupled Magnetic Resonators; 4×4 Transfer Matrix Method.
PACS numbers: 42.25.Ja; 78.20.Ls; 75.70.-i; 73.40.Gk

1. Introduction

Magnetooptical media have many potential applications, especially for the integration of magnetooptic isolator devices in photonic circuits because they may result in the development of smaller and cheaper isolators and circulators than presently possible [1 – 9]. Inoue et al. have demonstrated that an enhanced Faraday rotation takes place in one-dimensional (1D) magnetic photonic crystals with one defect composing of magnetooptical media [1 – 3]. The physical mechanism of Faraday rotation has been given in [4]. A linearly polarized light can be described as a combination of a right circular polarized light and a left circular polarized light. As the light passes through magnetooptical media, the right circular polarized light and the left circular polarized light undergo different phase shifts, respectively, which lead to the rotation of the polarization direction of the linearly polarized light. The resonant effect of the defect mode of 1D magnetic photonic crystals increases the Faraday rotation. Recently, we found that a slab of dielectric layer sandwiched between two identical metal slabs with negative-permittivity can achieve a resonant tunnelling [10]. In this structure, the electromagnetic fields in metal layers are evanescent. In general, evanescent waves can't propagate through a single dielectric layer. However, for the sandwiched structure, if the thickness of metal layer is very narrow, the evanescent field will be coupled into the dielectric layer and resonance between the two metal layers occurs. Thus the dielectric layer becomes a resonator. In order to utilize the effect of resonance, we change the dielectric resonator in the sandwiched structure as magnetic film resonator. Also, we add one more magnetic film and metal layer to the above structure to form two coupled magnetic resonators. Due to the unique transmission mechanism, the Faraday and Kerr effects of such structure take on a different form compared with those of conventional structures. Through numerical studies, an interesting phenomenon of split and merge of left–right-handed circular polarization light can be observed. Thus through our designed structure linear polarized light can be transformed into left-handed circular polarization light, right-handed circular polarization light or linear polarization light with arbitrary polarization direction.

© 2012 Verlag der Zeitschrift für Naturforschung, Tübingen · http://znaturforsch.com

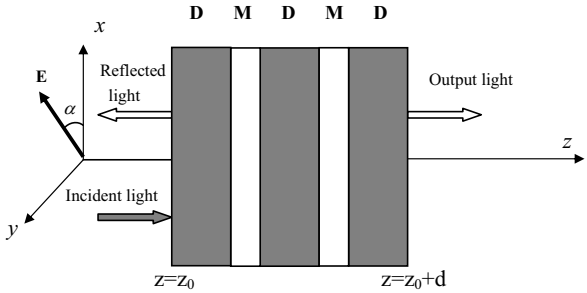

Fig. 1. Structure model: layers M are composed of magnetic material and layers D are composed of metal with negative permittivity.

2. Structure Model and Calculation Theory

The designed structure model is shown in Figure 1. A layered structure of DMDMD is placed along the z-axis in the background of air. Here D and M denote metal layers and magnetic layers with the thicknesses d_{D} and d_{M}, respectively. For the metal layers, the relative permittivity and permeability are given by

$$\varepsilon_{\mathrm{D}} = 1 - \omega_{\mathrm{ep}}^2/\omega^2, \;\; \mu_{\mathrm{D}} = 1\,. \tag{1}$$

Here ω_{ep} is the effective electronic plasma frequency and ε_{D} is negative when $\omega < \omega_{\mathrm{ep}}$. In general, the effective plasma frequency is a function of electron density and surface structure, such as subwavelength holes or slits, and can be tunable [11]. A monochromatic plane wave with angular frequency ω propagates in the direction of the z-axis with the electric field polarized in an arbitrary direction in the xy-plane having the specific form

$$\mathbf{E} = E_x \mathbf{e_x}\,\mathrm{e}^{\mathrm{i}(k_z z+\omega t)} + E_y \mathbf{e_y}\,\mathrm{e}^{\mathrm{i}(k_z z+\omega t)}\,, \tag{2}$$

where $\mathbf{e_x}$ and $\mathbf{e_y}$ are unit vectors along the x- and y-axis. The fundamental equations of light are given by Maxwell's equations:

$$\nabla \times \mathbf{E}(\mathbf{r}) = \mathrm{i}\,\omega\mu_0 \mathbf{H}(\mathbf{r})\,, \tag{3a}$$
$$\nabla \times \mathbf{H}(\mathbf{r}) = -\mathrm{i}\,\omega\varepsilon_0\tilde{\varepsilon}\mathbf{E}(\mathbf{r})\,, \tag{3b}$$

The specific dielectric tensor $\tilde{\varepsilon}$ in (3b) is given in (4) for the magnetic layers with the magnetizations parallel to the light propagation axis (Z-axis).

$$\tilde{\varepsilon} = \begin{bmatrix} \varepsilon_1 & \mathrm{i}\varepsilon_2 & 0 \\ -\mathrm{i}\varepsilon_2 & \varepsilon_1 & 0 \\ 0 & 0 & \varepsilon_3 \end{bmatrix}. \tag{4}$$

The value of ε_2 is dependent of the magnetizations and tunable. For the metal layers, we set $\tilde{\varepsilon} = \begin{bmatrix} \varepsilon_{\mathrm{D}} & 0 & 0 \\ 0 & \varepsilon_{\mathrm{D}} & 0 \\ 0 & 0 & \varepsilon_{\mathrm{D}} \end{bmatrix}$. To solve (4), it is convenient to use a state vector defined as $V(z) = [e_x, e_y, h_x, h_y]$. Here, $e_{x(y)}$ and $h_{x(y)}$ are the scaled $x(y)$-components of the electric and magnetic fields, respectively, which are introduced by the relations of $e_{x(y)} = \varepsilon_0 E_{x(y)}$ and $h_{x(y)} = E_{x(y)}/c$ with the vacuum dielectric constant ε_0 and the light vacuum velocity c. Taking (4) into (3), we obtain the following differential equation:

$$\frac{\mathrm{d}}{\mathrm{d}z} V(z) = C \cdot V(z) \tag{5}$$

where $C = \dfrac{2\pi\,\mathrm{i}}{\lambda} \begin{bmatrix} 0 & 0 & 0 & 1 \\ 0 & 0 & -1 & 0 \\ \mathrm{i}\varepsilon_2 & -\varepsilon_1 & 0 & 0 \\ \varepsilon_1 & \mathrm{i}\varepsilon_2 & 0 & 0 \end{bmatrix}$. Equation (5) has the eigensolution of $V(z) = V_0\,\mathrm{e}^{\lambda z}$. Taking $V(z) = V_0\,\mathrm{e}^{\lambda z}$ into (5), we obtain

$$(C - \lambda I)V_0 = 0\,. \tag{6}$$

Equation (6) is a matrix eigenequation and has four eigenvalues and four eigenvectors. Thus (5) has the general solution

$$\begin{aligned} V(z) = {} & A_1\mathbf{a}_1\,\mathrm{e}^{\mathrm{i}\lambda_1 z} + A_2\mathbf{a}_3\,\mathrm{e}^{\mathrm{i}\lambda_2 z} + A_3\mathbf{a}_3\,\mathrm{e}^{-\mathrm{i}\lambda_3 z} \\ & + A_4\mathbf{a}_4\,\mathrm{e}^{-\mathrm{i}\lambda_4 z}\,. \end{aligned} \tag{7}$$

Here $\mathbf{a}_i$ is the eigenvector corresponding to eigenvalue λ_i. Equation (7) can be written as

$$V(z) = \overline{a} \cdot \mathrm{e}^{\mathrm{i}\overline{\lambda} z} \cdot A\,, \tag{8}$$

where $\overline{a} = [a_1, a_2, a_3, a_4]$ is a 4×4 matrix, $A = [A_1, A_2, A_3, A_4]$, and

$$\mathrm{e}^{\mathrm{i}\overline{\lambda} z} = \begin{bmatrix} \mathrm{e}^{\mathrm{i}\lambda_1 z} & & & \\ & \mathrm{e}^{\mathrm{i}\lambda_2 z} & & \\ & & \mathrm{e}^{-\mathrm{i}\lambda_3 z} & \\ & & & \mathrm{e}^{-\mathrm{i}\lambda_4 z} \end{bmatrix}. \tag{9}$$

Equation (8) can be written as

$$\begin{aligned} V(z) &= \overline{a} \cdot \mathrm{e}^{\mathrm{i}\overline{\lambda}(z-z')} \cdot \overline{a}^{-1} \cdot \overline{a} \cdot \mathrm{e}^{\mathrm{i}\overline{\lambda} z'} \cdot A \\ &= P_l(z, z') \cdot V(z')\,, \end{aligned} \tag{10}$$

where $P_l(z, z') = \overline{a} \cdot \mathrm{e}^{\mathrm{i}\overline{\lambda}(z-z')} \cdot \overline{a}^{-1}$ is called 4×4 transfer matrix [1], and $l = D$ or M denotes the metal layer

or magnetic layer, z and z' are the positions of two interfaces of metal layer or magnetic layer. The state vector at incident interface $V(z=z_0)$ and at exit interface $V(z=z_0+d)$ follows the relation

$$V(z=z_0+d)=P_{\mathrm{D}}P_{\mathrm{M}}P_{\mathrm{D}}P_{\mathrm{M}}P_{\mathrm{D}}V(z=z_0)\,. \quad (11)$$

The angle between the direction of incident electric field polarization and the x-axis is denoted as α, and the amplitude of the incident electric field is normalized as one. Due to the nondiagonal item of $\tilde{\varepsilon}$, the incidence wave can result in another wave with the polarization direction perpendicular to that of the incidence wave. Thus the reflected and transmitted waves can be regarded as a superposition of the two waves with orthogonal polarization directions for the convenient of calculations. The state vector in the exterior space $z<z_0$ is given by the sum of the incident wave and the two reflected waves as

$$V(z)=\begin{bmatrix}\cos\alpha\\ \sin\alpha\\ -\sin\alpha\\ \cos\alpha\end{bmatrix}\mathrm{e}^{\mathrm{i}k(z-z_0)}+\left\{C_1\begin{bmatrix}\cos\alpha\\ \sin\alpha\\ \sin\alpha\\ -\cos\alpha\end{bmatrix}+C_2\begin{bmatrix}\sin\alpha\\ -\cos\alpha\\ -\cos\alpha\\ -\sin\alpha\end{bmatrix}\right\}\mathrm{e}^{-\mathrm{i}k(z-z_0)}\,, \quad (12)$$

and in the exterior space $z>z_0+d$ it is given by the sum of the two transmitted waves as

$$V(z)=C_3\begin{bmatrix}\cos\alpha\\ \sin\alpha\\ -\sin\alpha\\ \cos\alpha\end{bmatrix}\mathrm{e}^{-\mathrm{i}k(z-z_0-d)}+C_4\begin{bmatrix}\sin\alpha\\ -\cos\alpha\\ \cos\alpha\\ \sin\alpha\end{bmatrix}\mathrm{e}^{-\mathrm{i}k(z-z_0-d)}\,. \quad (13)$$

The values of C_1-C_4 are related with the amplitudes of the reflected and transmitted waves. We can obtain the values of C_1-C_4 just by taking (12) and (13) into (11). Thus the total state vector at output point $z=z_0+d$ can be decomposed in the x- and y-directions and is calculated through

$$V(z=z_0+d)=\begin{bmatrix}E_x\\ E_y\\ H_x\\ H_y\end{bmatrix}(z=z_0+d)=C_3\begin{bmatrix}\cos\alpha\\ \sin\alpha\\ -\sin\alpha\\ \cos\alpha\end{bmatrix}+C_4\begin{bmatrix}\sin\alpha\\ -\cos\alpha\\ \cos\alpha\\ \sin\alpha\end{bmatrix}\,. \quad (14)$$

From the total state vector the phase difference of $\mathbf{E}_x$ and $\mathbf{E}_y$ can be also obtained. Through (14), we can get the transmission properties of the model system.

3. Numercical Calculations and Analysis

In the numerical studies, without loss of generality, the structure parameters are set to be $\varepsilon_1=2$, $\omega_{\mathrm{ep}}=4\times10^{15}s^{-1}$, $d_{\mathrm{D}}=250$ nm, and $d_{\mathrm{M}}=600$ nm. In this case, if the frequencies $\omega<4\times10^{15}s^{-1}(\varepsilon_{\mathrm{D}}<0)$, the electromagnetic waves in layers D are evanescent fields. Through the coupling of evanescent fields, the periodic structure $(\mathrm{DM})^N\mathrm{D}$ (N is the period number) can become the coupled resonators and achieve a resonant tunnelling.

Firstly, we consider the simplest sandwiched structure DMD and set $\alpha=0$, $\varepsilon_2=0.05$. Figure 2a shows the reflection (left plots) and transmission spectra (right plots) and the corresponding phase difference $\Delta\phi$ ($\Delta\phi=\phi_x-\phi_y$) of $\mathbf{E}_x$ and $\mathbf{E}_y$ for the reflected (left plot) and transmitted waves (right plot). For the transmission wave, $\mathbf{E}_x$ and $\mathbf{E}_y$ have the same two resonant wavelengths at $\lambda_1=1042.65$ nm and $\lambda_2=1068.13$ nm with the same intensity value of 0.25. At λ_1 and λ_2, the phase differences are 0.5π and 0.5π, respectively. Thus the total state vectors at λ_1 and λ_2 are the left-handed circular polarization and the right-handed circular polarization, respectively. The trajectories of the end points of electric vectors at the two wavelengths are shown in Figure 2b. On the other hand, for the reflected wave the intensity spectrum of E_x^2 exactly drops at λ_1 and λ_2. Except for the two wavelengths, all the values of E_x^2 reach one, which means that the incident light undergoes intense reflection at other wavelengths. However, E_x^2 does not drop to zero and has the same value of 0.25 at the two wavelengths. It is interesting that the intensity spectrum of E_y^2 also has two peaks with the same value of 0.25 and the two peaks are

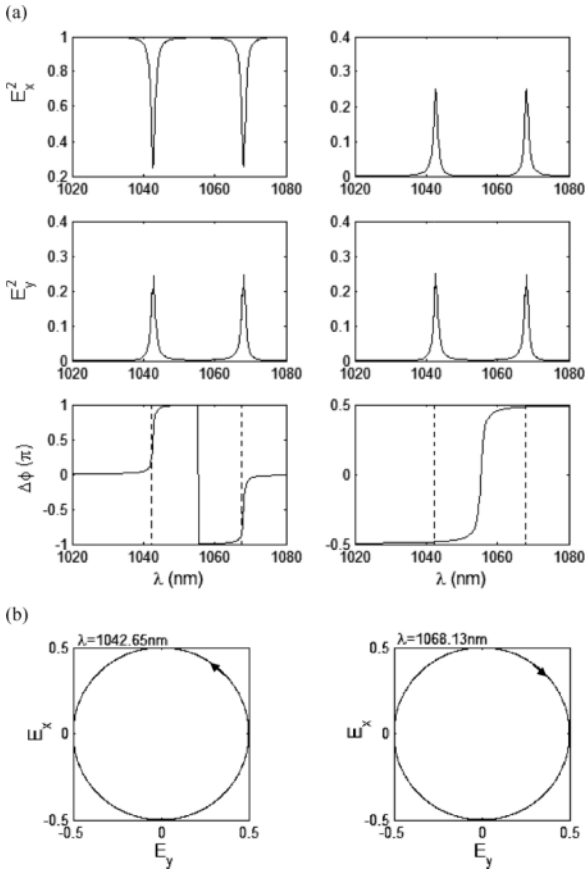

Fig. 2. (a) Reflection (left plots) and transmission spectra (right plots) of the structure DMD and the corresponding phase difference $\Delta\phi$ ($\Delta\phi = \phi_x - \phi_y$) of $\mathbf{E}_x$ and $\mathbf{E}_y$ for the reflected (left plot) and transmitted waves (right plot). The dotted line denotes the position of the resonant peak (α=0, $\varepsilon_2 = 0.05$). (b) Trajectories of end points of electric vectors at two wavelengths.

exactly at the two wavelengths λ_1 and λ_2. It is noted from Figure 2 that at λ_1 and λ_2 the phase differences are 0.5π and -0.5π, respectively. Thus the total state vectors of the reflected wave at λ_1 and λ_2 are the right-handed circular polarization and the left-handed circular polarization, respectively. The total intensity at one wavelength is the sum of E_x^2 and E_y^2. It is noted that at any wavelength the total intensity of the reflected and transmitted waves keeps one due to the conservation of energy.

One may ask what leads to the unique results. We think that they are attributed to both of the magnetooptical effect and the intense resonant effect. As we have known, linearly polarized light can decompose into one left-handed circular polarization and one right-handed circular polarization. The left-handed circular polarization and the right-handed circular polarization have the same refraction index and undergo the same phase shift in isotropic media. Thus linearly polarized light has no polarization change when it passes through isotropic media. However, the permittivities in magnetooptical media are $\varepsilon_r = \varepsilon_1 + \varepsilon_2$ for the right-handed circular polarization and $\varepsilon_l = \varepsilon_1 - \varepsilon_2$ for the left-handed circular polarization [4]. Thus the refraction indices for the two polarizations are different and the two polarizations undergo different phase shifts when the light passes through magnetooptical media, which results in a rotation of polarization called the Faraday and Kerr effect. The Faraday effect can be increased in one-dimensional photonic crystals with defects composed of magnetooptical materials and has been studied widely [1–9]. However, for the structure model in this study, the Faraday effect and Kerr effect takes on a different form. At λ_1, the incident linearly polarized light becomes a transmitted left-handed circular polarization and reflected right-handed circular polarization with the same intensity. On the other hand, at $\lambda_2 = 1053.188$ nm, the incident linearly polarized light becomes a transmitted right-handed circular polarization and reflected left-handed circular polarization with the same intensity. One may still ask what leads to the structure having the unique function. The current DMD structure can be looked at as a resonant cavity. Only if the light satisfies the resonant condition, it can be transmitted through the structure. The resonant condition is very sensitive to the change of the refraction index of layer M. At λ_1, it is the left-handed circular polarization with $\varepsilon_l = \varepsilon_1 - \varepsilon_2$ that satisfies the resonant condition. Therefore, for an incidence of linearly polarized light, the left-handed circular polarization can pass the structure, while the right-hand circular polarization is reflected. At λ_2, it is the right-handed circular polarization that satisfies the resonant condition. Therefore, the right-handed circular polarization can pass the structure, while the left-handed circular polarization is reflected. Therefore, the current DMD structure can be understood as a splitter of polarizations, which decomposes linearly polarized light into two circular polarizations with reversal rotation directions.

Now, we consider the effect of ε_2. Basing on the structure parameters of Figure 2, we show the trans-

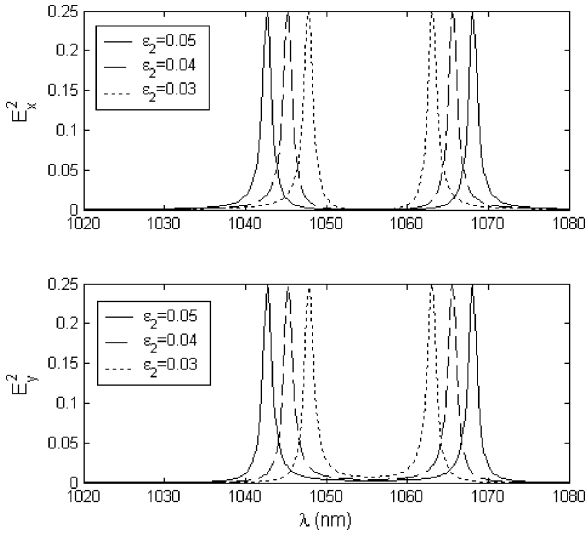

Fig. 3. Transmission spectra of the structure DMD for different values of $\varepsilon_2(\alpha = 0)$.

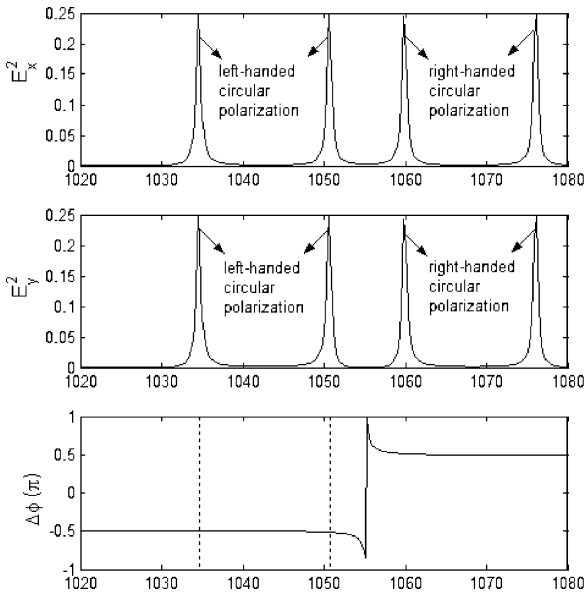

Fig. 4. Transmission spectra and the corresponding phase difference $\Delta\phi$ for structure DMDMD. The dotted line denotes the position of the resonant peak. The structure parameters are the same as those of Figure 2.

mission spectra for different values of ε_2 in Figure 3. It is clear that the value of ε_2 determines the wavelength interval between the two circular polarizations. The less the value of ε_2, the smaller the wavelength interval.

Secondly, we consider the structure DMDMD. The structure parameters are the same as those of Figure 2. The transmission spectra and the corresponding phase difference $\Delta\phi$ for $\alpha = 0$ are shown in Figure 4. There are the same four resonant wavelengths with the same intensity value of 0.25 corresponding to $\mathbf{E}_x$ and $\mathbf{E}_y$. For the left two resonant wavelengths the phase differences are -0.5π, while for the right two resonant wavelengths the phase differences are -0.5π and 0.5π, respectively. Thus the total state vectors at the left two resonant wavelengths and the right two resonant wavelengths are the left-handed circular polarization and the right-handed circular polarization, respectively. Compared with Figure 2, the only difference in Figure 4 is that the single resonant wavelength is split into two resonant wavelengths with the same polarization. The split of the resonant peak is due to the coupling of the resonators. There are two resonators M in the structure DMDMD. Because layer D is very narrow, the energy in the former resonator can be tunnelled to the latter resonator through the evanescent field within layer D. Thus a coupling between the two resonators occurs. According to the tight-binding model (TBM) in solid physics, one atom energy level is split into N levels when N atoms are combined. The photonic version of TBM for dispersive photonic systems, particularly in plasmonic materials and optical metamaterials, has been established in [12]. According to [12], the split number of the resonant peak is just equal to the number of resonators. The results for more resonators in the structure DM…DMD are verified through our calculations. In this paper, we focus on the structure DMDMD.

If we decrease the value of ε_2, the two left resonant peaks and the two right resonant peaks close up to each other. Thus an interesting result will occur, i. e., the inner two peaks will be merged into one peak. To give a specific result, we show the transmission spectra for $\varepsilon_2 = 0.0315$ and $\alpha = 0$ in Figure 5. The other parameters are the same as those of Figure 4. It is noted from Figure 5 that the two outside resonant peaks move to 1039.255 nm and 1071.35 nm and still correspond to the left-handed circular polarization and the right-handed circular polarization, respectively, but the inner two peaks have been merged into one peak at the same wavelength 1055.31nm. For the electric fields $\mathbf{E}_x$ and $\mathbf{E}_y$, the phase difference $\Delta\phi$ at the middle peak is equal to zero, which means that the light at the middle peak becomes a linear polarization. The linear polar-

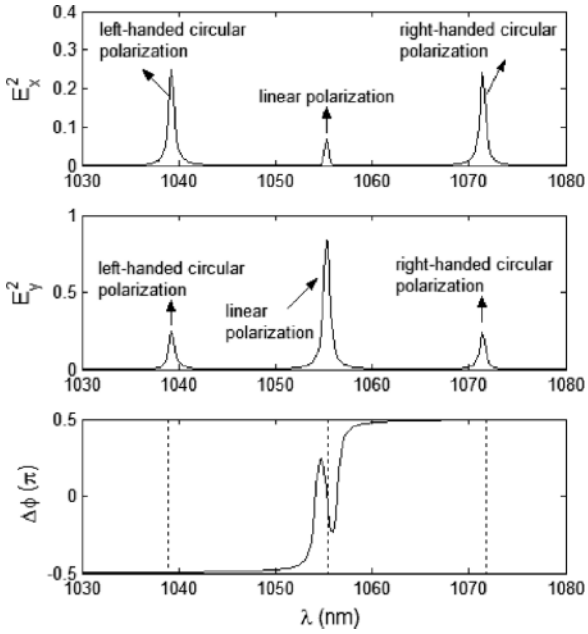

Fig. 5. Transmission spectra and the corresponding phase difference $\Delta\phi$ for structure DMDMD and $\varepsilon_2 = 0.0315$. The other structure parameters are the same as those of Figure 2. The dotted line denotes the position of the resonant peak.

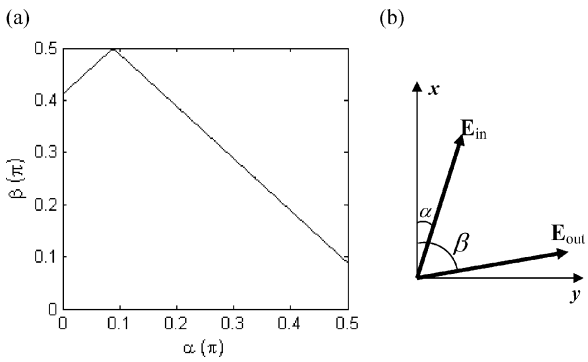

Fig. 6. Dependence of β on α (left plot). Here β denotes the angle between the polarization direction of the output linearly polarized light and the x-axis. The right plot is the schematic of the incident electric field vector and the output electric field vector.

ization has a total intensity of 0.9418. Thus the incidence of linearly polarized light can output light with three kinds of polarizations through the coupled magnetic resonators.

Here, we study the effect of α on the polarizations. We find that the value of α has no effect on the two outside circular polarizations and the intensity of the middle peak. However, the polarization direction of the output linearly polarized light is sensitive to the value of α. We use β to denote the angle between the polarization direction of the output linearly polarized light and the x-axis. According to $\beta = \arctan(E_y/E_x)$, we obtain the dependence of β on α, which is shown in Figure 6. There are two straight lines in the figure. For $\alpha = 0$, 0.09π, and 0.5π, β is equal to 0.41π, 0.5π, and 0.09π, respectively. For $\alpha < 0.09\pi$, the value of β increases linearly with the value of α, while for $\alpha > 0.09\pi$, the value of β decreases linearly with the value of α. Thus through changing the value of α, we can arbitrarily control the polarization direction of the output linearly polarized light in the range of $0.09\pi \leq \beta \leq 0.5\pi$. Hao et al. have achieved manipulating reflected electromagnetic wave polarizations by anisotropic metamaterials [13, 14]. Later Sun et al. designed an anisotropic metamaterial to manipulate EM wave polarizations in transmission geometry [15]. Mutlu and Ozbay also reported a three-layer ultrathin chiral metamaterial that rotates the polarization plane of an incident linearly polarized wave by 90° with unit transmittance independent of the polarization angle [16]. All the above published works are based on the design of anisotropic metamaterial or chiral metamaterial. In this work, we only use isotropic metamaterial and magnetic material in the designed structure to control the polarization direction of the linearly polarized light.

4. Conclusions

In this paper, we designed coupled magnetic resonators. We study the transmission properties by a numerical method. The incidence linearly polarized light can be spilt into a left-handed circular polarization and a right-handed circular polarization for one magnetic resonator. Both the left-handed circular polarized light and the right-handed circular polarized light are further split into two resonant peaks for the two-coupled magnetic resonators. Through adjusting the magnetizations, the inner left-handed circular polarization and right-handed circular polarization can be merged into one linear polarization, while the two outside resonant peaks keep circular polarized. Thus the incidence of linearly polarized light can be tranformed in output light with three kinds of polarizations through the coupled magnetic resonators. Our studies may provide a new means of controlling light polarizations in future optical devices.

[1] M. Inoue, K. Arai, T. Fujii, and M. Abe, J. Appl. Phys. **83**, 6768 (1998).
[2] M. Inoue and T. Fujii, J. Appl. Phys. **81**, 5659 (1997).
[3] M. Inoue, K. Arai, T. Fujii, and M. Abe, J. Appl. Phys. **85**, 5768 (1999).
[4] H. Kato, T. Matsushita, A. Takayama, M. Egawa, K. Nishimura, and M. Inoue, J. Appl. Phys. **93**, 3906 (2003).
[5] E. Takeda, N. Todoroki, Y. Kitamoto, M. Abe, M. Inoue, T. Fujii, and K. Arai, J. Appl. Phys. **87**, 6782 (2000).
[6] S. Sakaguchi and N. Sugimoto, J. Lightwave Technol. **17**, 1087 (1999).
[7] M. J. Steel, M. Levy, and R. M. Osgood Jr., IEEE Photon. Technol. Lett. **12**, 1171 (2000).
[8] M. J. Steel, M. Levy, and R. M. Osgood Jr., J. Lightwave Technol. **18**, 1289 (2000).
[9] M. J. Steel, M. Levy, and R. M. Osgood Jr., J. Lightwave Technol. **18**, 1297 (2000).
[10] G. Yu and Y. Fang, Opt. Laser Technol. **43**, 36 (2011).
[11] J. B. Pendry, L. Martín-Moreno, and F. J. Garcia-Vidal, Science **305**, 847 (2004).
[12] B. Xi, H. Xu, S. Y. Xiao, and L. Zhou, Phys. Rev. B **83**, 165115 (2011).
[13] A. Raman and S. Fan, Phys. Rev. Lett. **104**, 087401 (2010).
[14] J. Hao, Y. Yuan, L. Ran, T. Jiang, J. A. Kong, C. T. Chan, and L. Zhou, Phys. Rev. Lett. **99**, 063908 (2007).
[15] W. Sun, Q. He, J. Hao, and L. Zhou, Opt. Lett. **36**, 927 (2011).
[16] M. Mutlu and E. Ozbay, App. Phys. Lett. **100**, 051909 (2012).